TMS 2018: 147h Annual Meeting & Exhibition

Symposium – Additive Manufacturing of Metals: Establishing Location Specific, Processing Microstructure-Property Relationships III; Session – High Temperature Alloys and Properties

Location-specific microstructure and the effect of heat treatment on electron-beam melted Ni-based superalloy LSHR

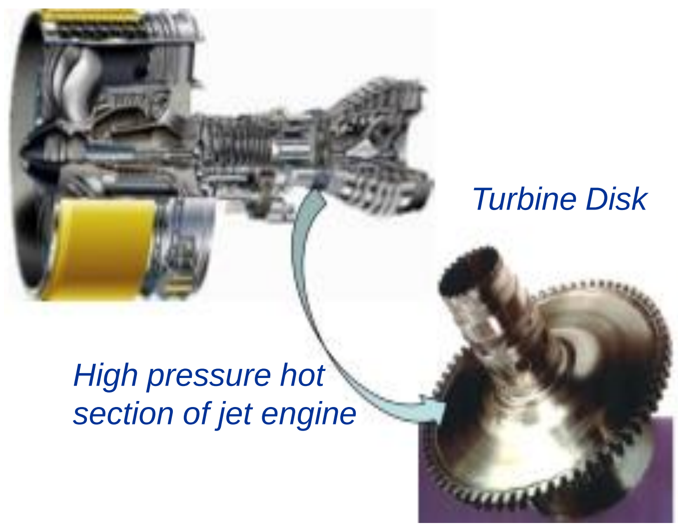

Chantal K. Sudbrack[1,*]; Michael M. Kirka[2]; S. Lee Semiatin[3]; Timothy P. Gabb[1]

1. NASA Glenn Research Center (Cleveland OH)

* *Separated Early 2018*

2. Oak Ridge National Laboratory (Oak Ridge TN)

3. Air Force Research Laboratory (WPAFB OH)

Acknowledgements: *ORNL's Manufacturing Demonstration Facility for EBM fabrication. Quintus Technologies for Pressurized Heat Treatment. Peter Bonacuse, Rick Rauser, Dereck Johnson, Rick Rogers, Joy Buehler support of NASA GRC for experimental and analytical support; Holly Sirk and Bethany Cook of Case Western Reserve University for intern support. NASA MSFC's AM facility for SLM trials.*

Funding: *NASA GRC Center Innovation Fund, NASA HEOMD Additive Manufacturing Structural Integrity Initiative, DOE Office of Energy Efficiency & Renewable Energy, Advanced Manufacturing Office, contract DE-AC05-00OR22725 with UT-Battelle, LLC.*

March 13, 2018

The γ’-strengthened Ni-based superalloys are used in demanding, high-temperature environments in gas turbine engines for aviation

50 % or more of the engine weight is from nickel alloys

Turbofan

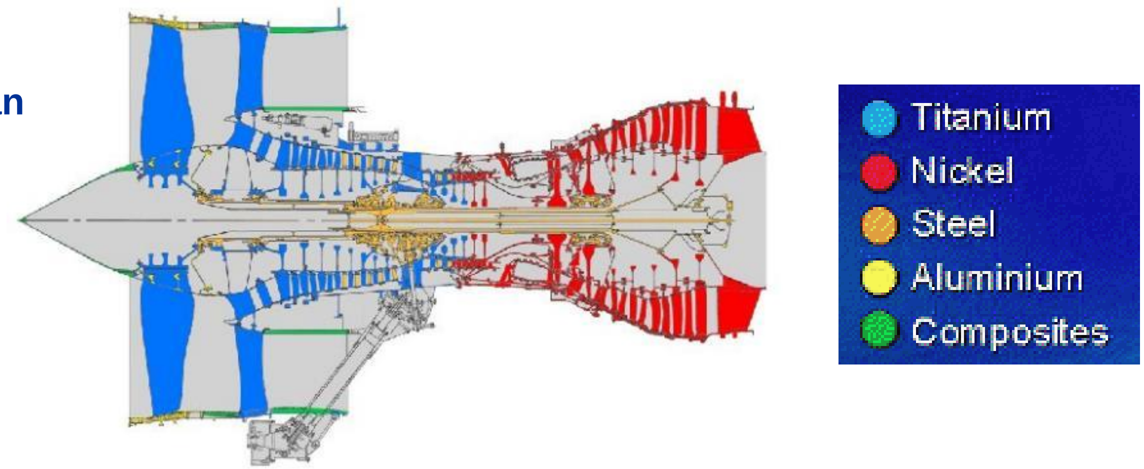

Other turbomachinery applications:

- **Next generation nuclear reactors**
- **Land based gas power generation**
- **Turbopumps for rocket engines**
- **Marine gas engines**

Scale down of blades in gas turbines

- *Investment casting cost effective for high production (100,000 parts / year)*
- *Target low production to avoid custom made tooling & intricate structures*
- *Target cooling efficiency, intricate net-shape with **precision powder-bed AM***

Metals AM is rapidly advancing. To move beyond common alloys needs R&D.

Goal: Use LSHR as a gateway towards fabrication for other Ni-based γ'-superalloys

Superalloy weldability map

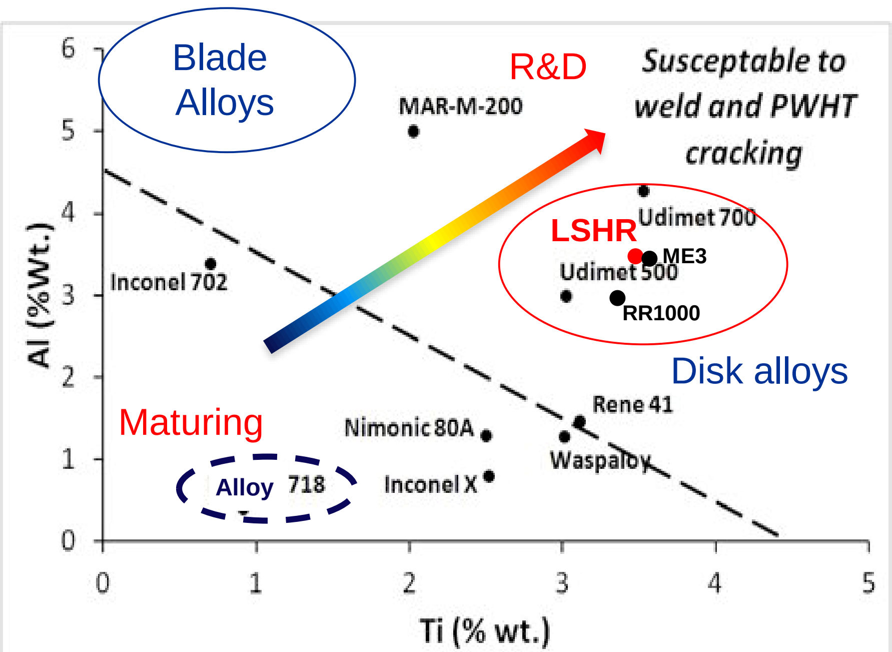

Cracking observed in our SLM trials

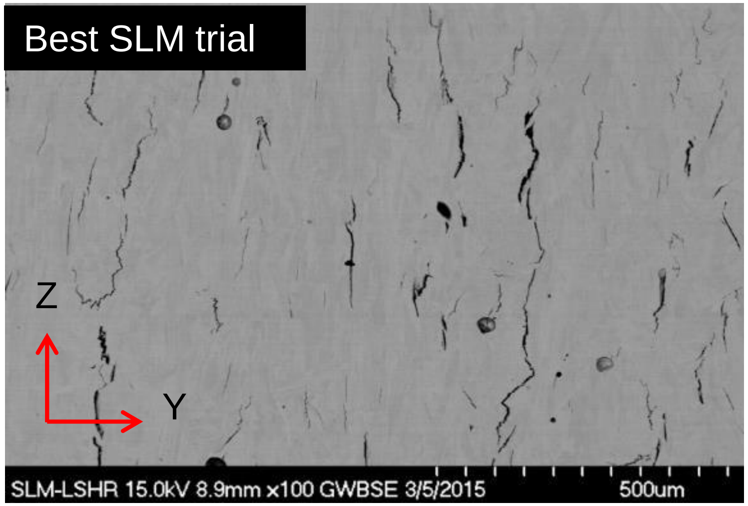

Selective laser melting *(SLM) →*
Thermal-induced cracking due to steep thermal gradients between melt pools

Prior Work: Established **low porosity** & **crack-free** LSHR with Electron Beam Melting

- Heated-bed (> 900 ºC) leads to less steep gradients between melt pools for EBM

Aim: Understand post-processing heat treatment & location-specific microstructure

Benchmark with state of the art

PM disk application targets strength, creep, and fatigue

Heat treated <u>L</u>ow-<u>S</u>olvus <u>H</u>igh <u>R</u>efractory (LSHR) PM alloy

γ’

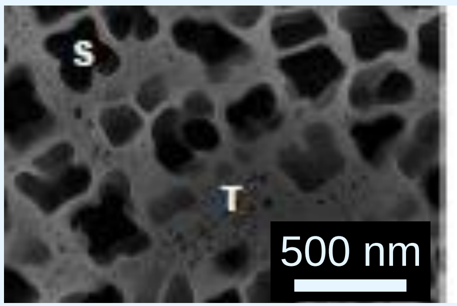

Equiaxed grains, d= 15–50 µm

Cr,Mo,Co-rich $M_{23}C_6$ carbides
- ornament GBs

Ti,Ta,Nb-rich MC and M_3B_2
- interior & GBs

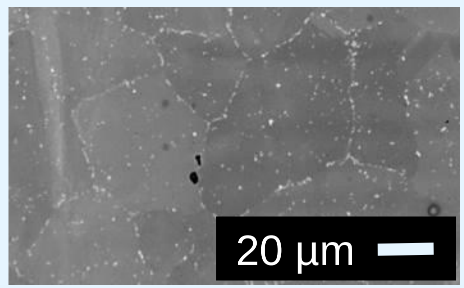

<u>γ’-Ni_3(Al,Ti) precipitates</u>

Volume Fraction: ~55%

Secondary γ’ : d= 200–350 nm

Tertiary γ’ , d= 20–40 nm

Patent US 6974508 B1, 2005, NASA/TM-2005-213645

PM Mechanical Properties

Normalized Life/Strength

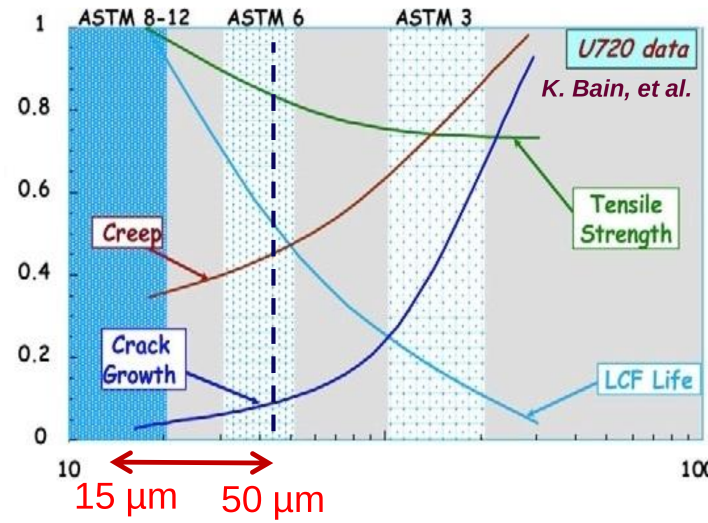

What are the grain sizes for EBM LSHR?

Nominal

wt.%	Cr	Co	Al	Ti	Nb	Ta	Mo	W	Zr	C	B	trace	Ni
NASA LSHR	12.5	20.5	3.5	3.5	<u>1.5</u>	<u>1.5</u>	<u>2.7</u>	<u>4.3</u>	0.05	0.05	0.03	Si, Fe, N, O, S	bal

10 wt% refractory elements

Oak Ridge National Laboratory

Objectives

- Examine set-to-set variability with 4 build sets with the same layout
- Establish the effect of solutioning heat treatments (HT) on as-fabricated grain structure and microstructure – γ'-solvus= 1156 ºC
  - (1) As-fabricated
  - (2) 2 hour subsolvus HT(-15 ºC) + conventional 2-step aging
  - (3, 4, 5) 0.5 hour, 2 hours, 4 hours supersolvus HT (+18 ºC) + 2 step aging
- Gain insight into location-specific microstructure to correlate later to mechanical properties (tensile, creep, LCF behavior)

Outline

- About the EBM Builds
- Results:
  - Composition
  - As-fabricated grain structure → Deep Dive
  - Solidification observations
  - Minor phases
  - Heat-treatment response
- Concluding remarks and future work

LSHR EBM Builds at ORNL MDF

EBM fabrication at MDF

Arcam S12 (modified A2-like)

- Stainless steel substrate
- EBM powder cut: 45-106 µm
- Pre-heats/ Re-heats: **900-1100 °C**
- Continuous snaking scan strategy
- **90 µm layer thicknesses**
- < 5 x10^{-3} Torr of He

(1) "Short" In-plane Rectangular Blanks

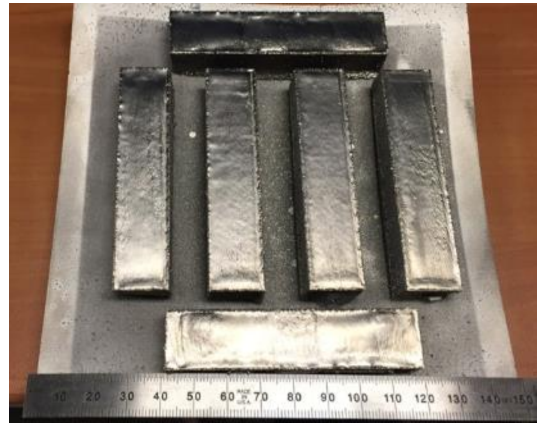

16 mm x 79 mm x 18 mm

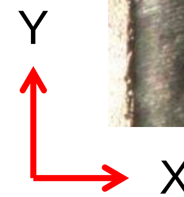

CTE differences led to warping of SS plate with several mm deflection

4 build sets with this layout

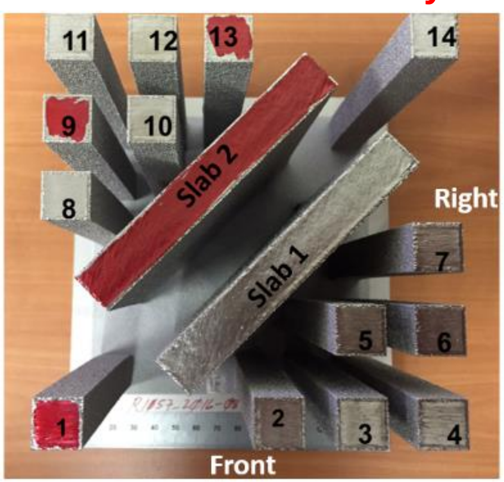

(2) Four identical build sets with Z-direction Rectangular Blanks & Slabs for In-Plane Blanks

- 14 Z-bars: vertical rectangular blanks in the build direction
- Each slab allows up to 6 in-plane blanks (12 total per set)

CT scans Defect free	Set 1	Set 2	Set 3	Set 4
Z-bars	14/14	14/14	14/14	14/14
In-plane (Slab)	6/12	12/12	12/12	11/12

Z-bar: 15 mm x 15 mm x 95 mm, Slab: 15 mm x 95 mm x 95 mm

Z is the build direction, Y is perpendicular to scan, while X is parallel

Build Set Comparison

Composition: Excellent Agreement within Build & Build-to-Build

Major Element	Build-to-Build	Upper-to-Lower	Upper: 15 mm beneath top surface					Lower: 15 mm above build plate					Powder (wt.%)	Delta (wt.%)	Major Element
			Set 1	Set 2	Set 3	Set 4	Average	Set 1	Set 2	Set 3	Set 4	Average			
Al	✔	✔	3.50	3.51	3.51	3.52	3.51	3.50	3.50	3.50	3.52	3.51	3.50	✔	**Al**
Co	✔	✔	20.43	20.43	20.44	20.40	20.42	20.44	20.41	20.42	20.39	20.41	20.56	**0.15 ↓**	**Co**
Cr	✔	✔	12.11	12.14	12.20	12.12	12.14	12.16	12.14	12.20	12.07	12.14	12.35	**0.21 ↓**	**Cr**
Fe	✔	✔	0.015	0.016	0.016	0.015	0.015	0.015	0.016	0.018	0.016	0.016	0.013	✔	**Fe**
Mo	✔	✔	2.76	2.75	2.74	2.76	2.75	2.74	2.75	2.73	2.78	2.75	2.74	✔	**Mo**
Nb	✔	✔	1.53	1.52	1.51	1.52	1.52	1.52	1.52	1.51	1.53	1.52	1.51	✔	**Nb**
Ni	✔	✔	49.9	50.0	49.9	49.9	49.9	50.0	49.9	50.0	49.9	49.9	49.6	bal	**Ni**
Ta	✔	✔	1.47	1.47	1.48	1.52	1.48	1.47	1.49	1.48	1.53	1.49	1.59	**0.10 ↓**	**Ta**
Ti	✔	✔	3.54	3.53	3.51	3.53	3.52	3.52	3.53	3.51	3.55	3.52	3.48	✔	**Ti**
W	✔	✔	4.48	4.48	4.45	4.49	4.47	4.46	4.48	4.45	4.50	4.47	4.49	✔	**W**
Minor Element (Trace)															Minor Element (Trace)
B	✔	✔	0.050	0.045	0.050	0.050	0.049	0.050	0.050	0.050	0.050	0.050	0.020	**0.030 ↑**	**B**
C	✔	✔	0.038	0.038	0.038	0.039	0.038	0.038	0.039	0.039	0.038	0.038	0.040	✔	**C**
O (ppm)	~	✔	45	89	87	85	76	86	56	101	57	75	110	**35 ↓**	**O (ppm)**
Si	~	~	0.030	0.035	0.040	0.040	0.036	0.035	0.050	0.060	0.040	0.046	0.021	**0.022 ↑**	**Si**
Zr	✔	✔	0.085	0.085	0.085	0.083	0.084	0.086	0.084	0.088	0.084	0.085	0.040	**0.044 ↑**	**Zr**

✔ Agreement ~ Some variability Depletion Enrichment

- Powder chemistry agrees with EBM builds for Al, Fe, Mo, Nb, Ti, W, and C
- Builds are slightly depleted in Co, Cr, Ta but still within specification for LSHR
    - 33% reduction in oxygen content in builds likely due to loss of absorbed oxygen from surfaces of powder particles

As-fabricated builds have very elongated needle-shaped grains in the build direction

Short In-Plane Blank

Zone I: Top volume with few passes of e-beam has finer γ'-precipitates (diameter= 90-120 nm)

Zone 2: Interior volume with multiple reheats and sustained heat (γ'-cube length= 240-360 nm)

Zone 3: Strained volume adjacent to build plate with interdiffusion from plate

Interior – (001) Texture

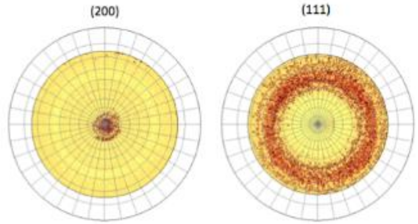

Interior Near Edge

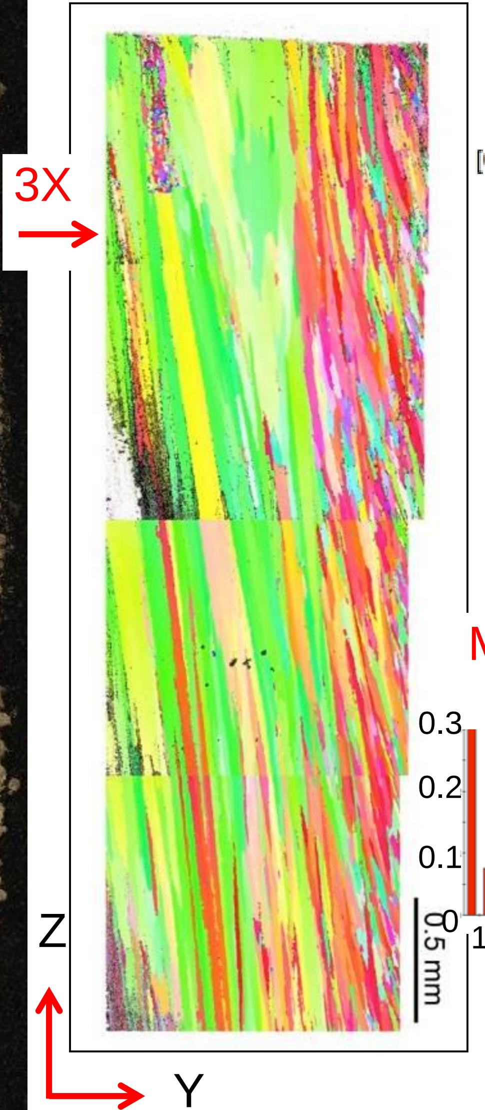

Inverse pole figure

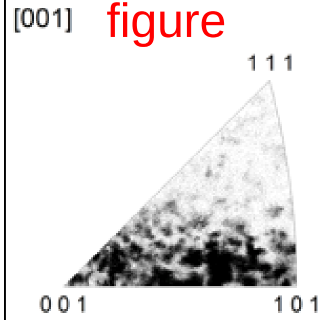

Misorientation angle

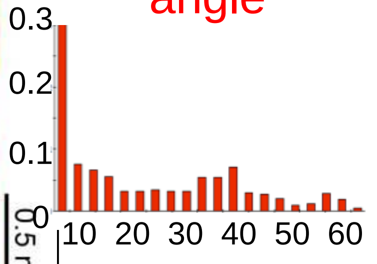

Hot time, multiple passes, and substrate strain effects

Short In-Plane Blank

Grain boundaries are stabilized by γ'-precipitates

Mid slice

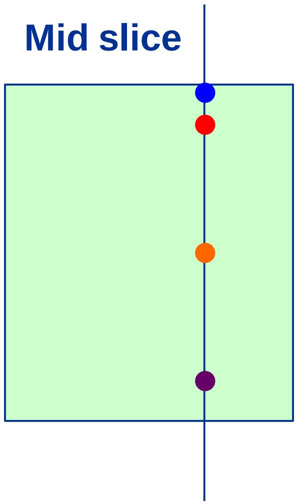

- Top (zone1)
- Top (zone2)
- Mid (zone2)
- Bot (zone3)

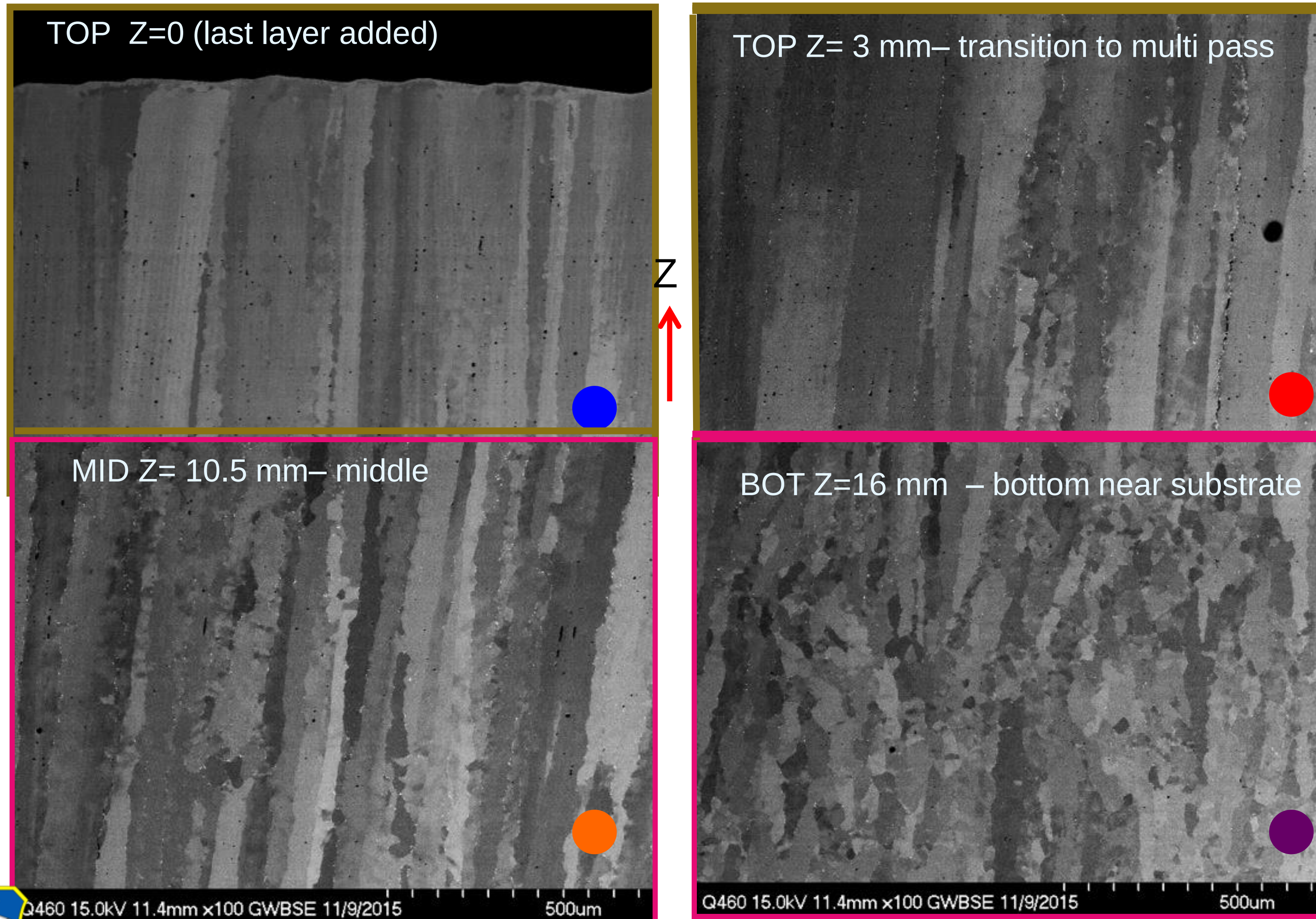

Grain boundaries stabilized by minor phases

As-fabricated: Map grain structure in build direction (Zone 2)

Vertical Z-bar Blank

15 x 15 x 95 mm^3

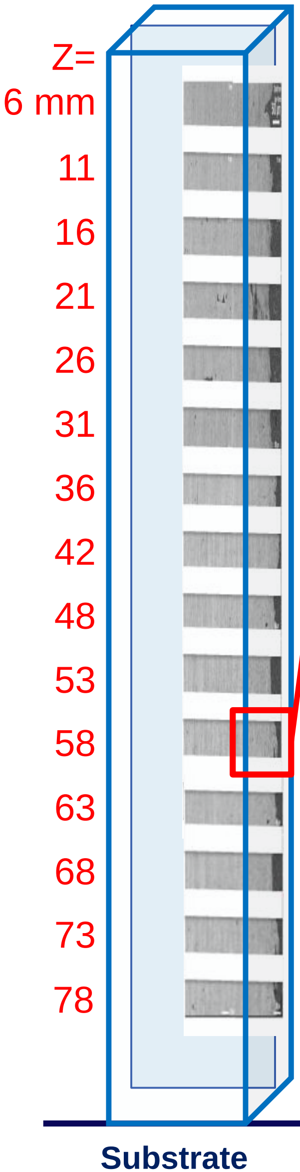

Transverse Grain Widths: Measure lineal intercept across in three areas for each Z

Zone 2: each layer experiences multiple passes of E-beam

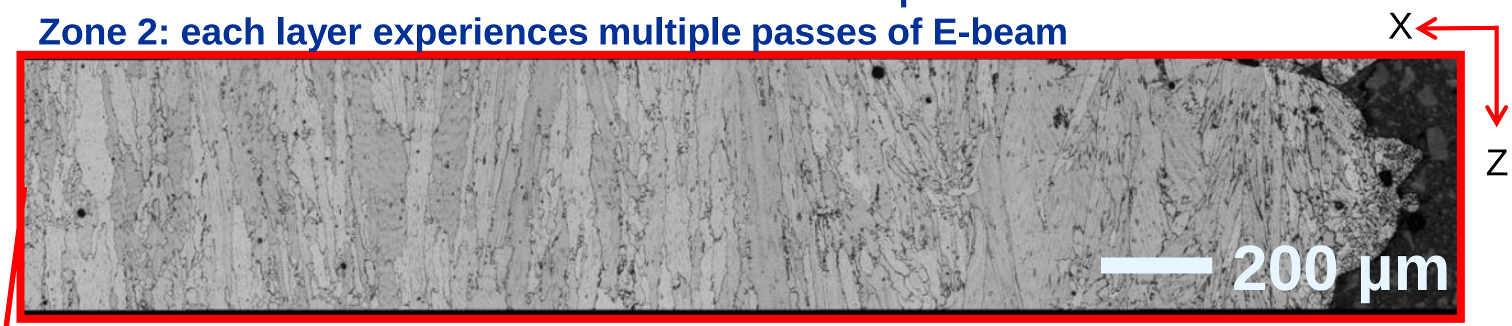

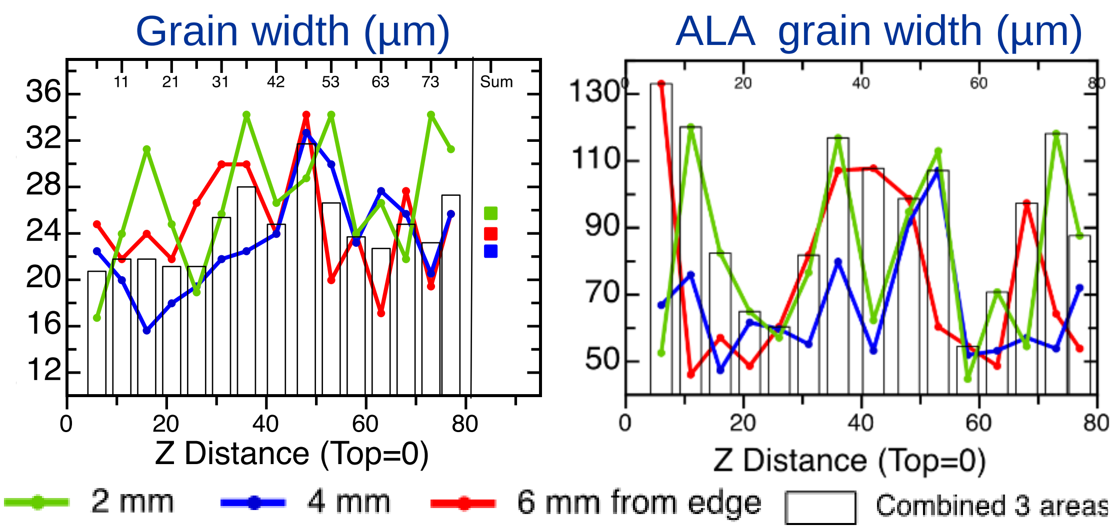

2X-5X larger ALA than the overall average width

- **Overall average AF grain width: 24 ± 2 µm**
- **For constant Z, grain widths show up to 2X scatter** between 2 mm, 4 mm, 6 mm areas yet similar trends
- **Arch shape with Z** for combined data: Highest values observed for the middle of the bar

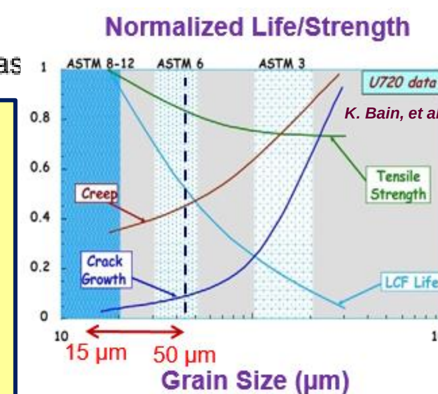

Solidification-induced segregation of fine dendrites

Short In-Plane Blanks: EPMA maps of transverse interior area

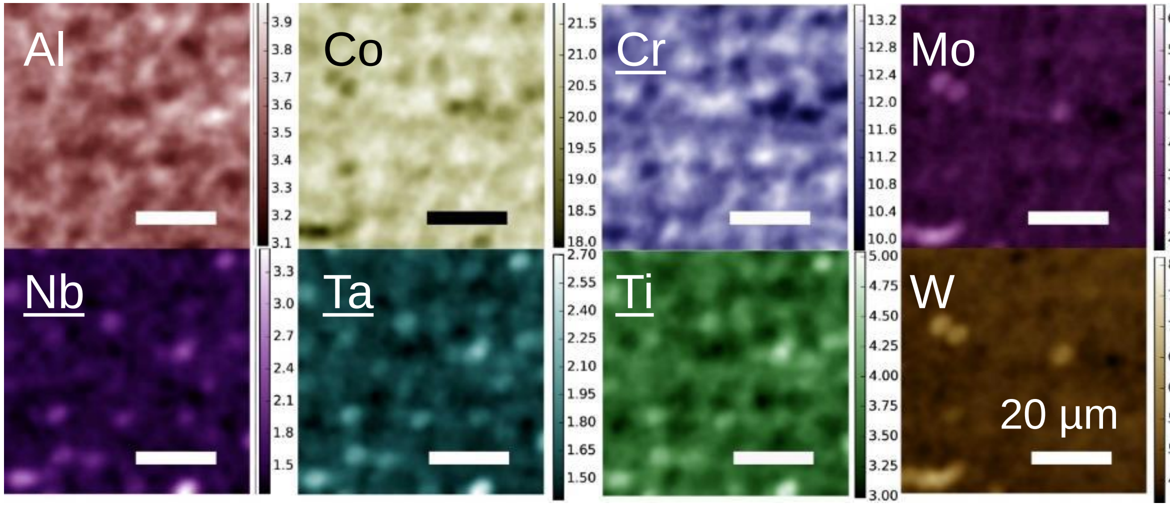

Z

Cores identified with Cr map

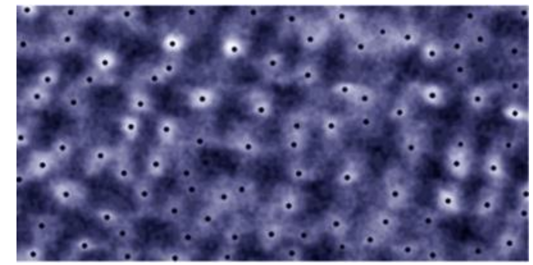

91 cores λ= 10.1 ± 0.6 µm

Est. cooling rate= $5x10^3$ ºC/s

- Finely spaced with primary dendrite arm spacing (λ) of 10.1 ± 0.6 µm, which is 20X smaller than what may be observed for a casting
- Dendrite cores: Cr and Co rich, to smaller extent Mo, W
- Interdendritic regions: Al, Nb, Ta, Ti rich
- The compositions of the Regions of interest (ROI) are used to predict ROI γ'-solvus temperature and γ'-volume fraction

JMatPro8-Nidat7 γ'	ΔTsol	Vf (%)
Core-blanks	–13 ºC	53.2
InterD-blanks	+14 ºC	*58.7*

Microstructure similar to conventionally processed LSHR

Heated-bed leads to coarsening of minor phases at GBs

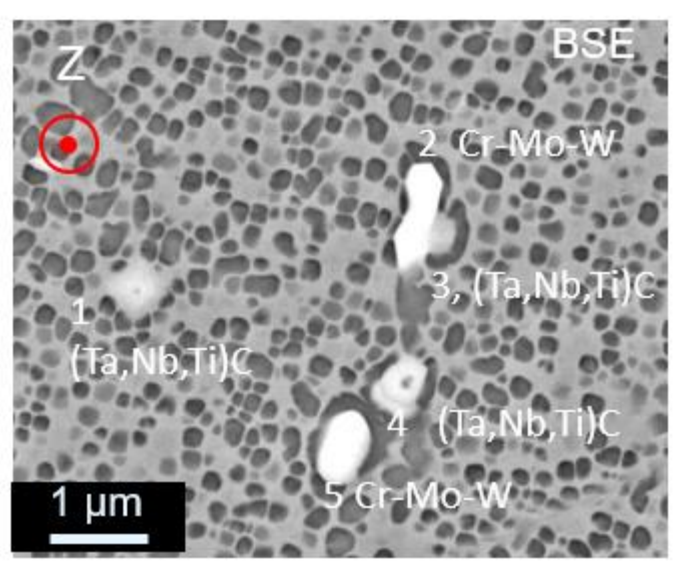

As-fabricated:

$(Cr,Mo)_{23}C_6$ are predicted to be unstable at 937 ºC

DTA liquation temperatures for as-forged PM LSHR

Stable to high HTs:

$T_m[(Cr,Mo)_3B_2]$= 1202 ºC

$T_m[(Ti,Ta,Nb)C]$= 1310 ºC

TP Gabb, CK Sudbrack et al.
NASA/TM–2012-217604 (2012)

Larger carbides re-solution during high temperature solutioning

Differential Thermal Analysis: PM vs. EBM

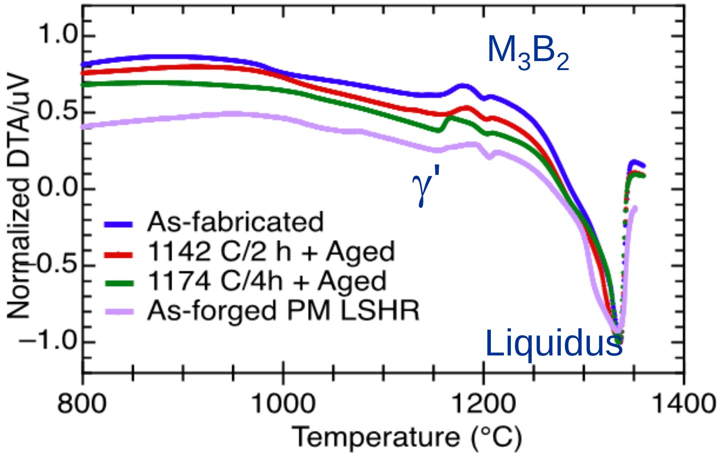

As-fabricated **2 h Supersolvus HT**

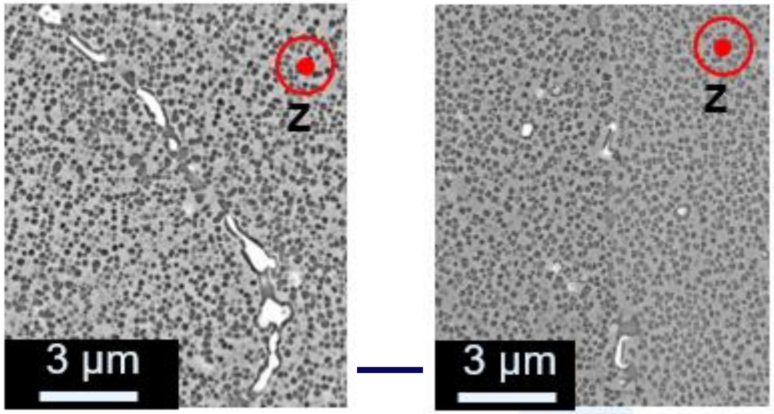

Center Slab – Longitudinal Grains in Z

Recrystallization & modest grain growth during supersolvus HT

As-Fabricated	Subsolvus HT (-15ºC) for 2h + Aging	Supersolvus HT (+18ºC) for 0.5 h + Aging	Supersolvus HT (+18ºC) for 2 h + Aging	Supersolvus HT (+18ºC) for 4 h + Aging

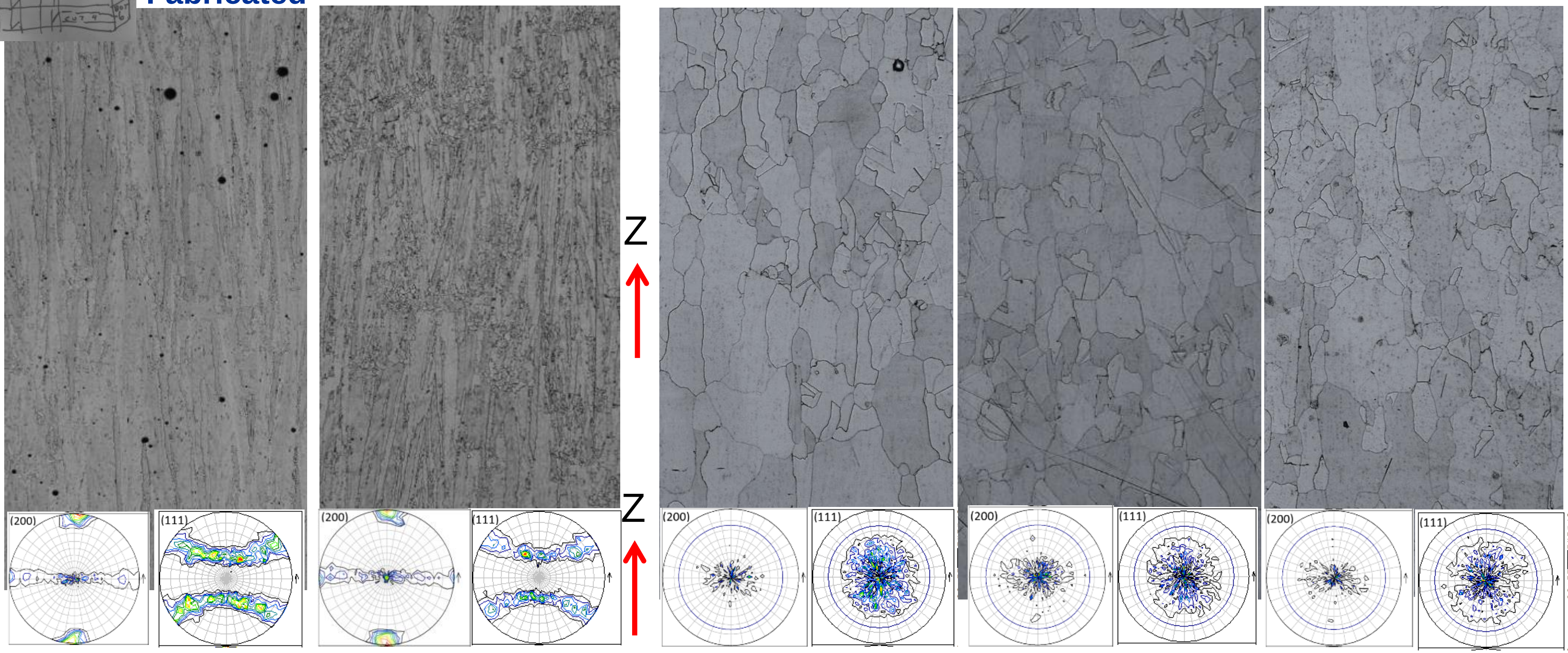

Etch micrographs and XRD pole figures similar near edge

500 µm

Z-bar – Transverse Grain Traces

Avg. Feret Diameter	AF	Sub 2 h	Sup 0.5 h	Sup 2 h	Sup 4 h
Upper	21 µm	38 µm	67 µm	79 µm	88 µm
Lower	35 µm	37 µm	85 µm	93 µm	107 µm

Chemical banding produces bimodal γ'-distributions for subsolvus HT

As-Fabricated

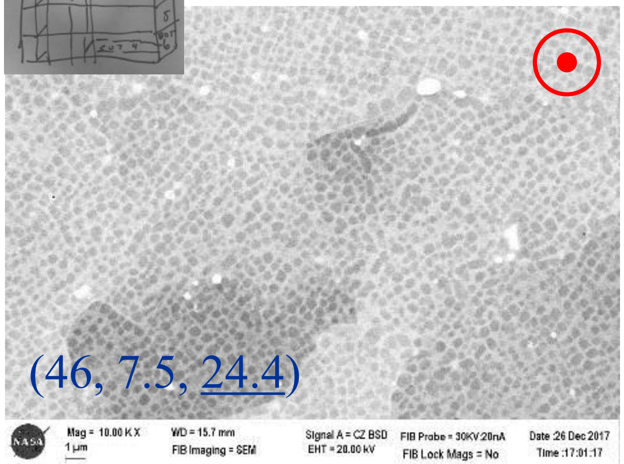

Subsolvus HT (-15ºC) for 2h + Aging

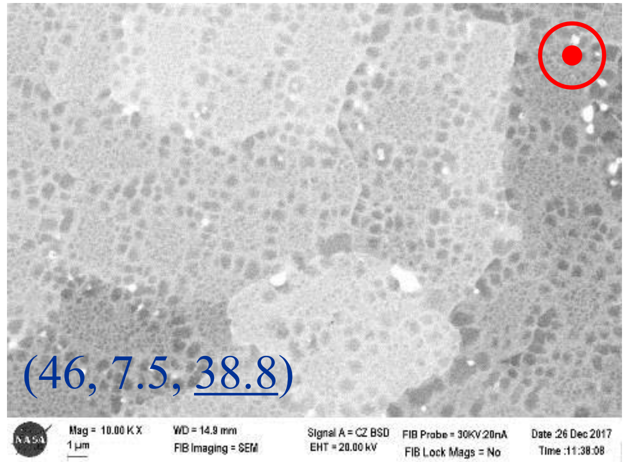

- **Subsolvus: Precipitates at the GBs stabilize grains**
- **Supersolvus: Exhibits modest grain growth with increased hold time**

JMatPro8-Nidat7	ΔTsol	Vf (%)
Core-blanks	–13 ºC	53.2
InterD-blanks	+14 ºC	*58.7*

Supersolvus HT (+18ºC) for 0.5 h + Aging

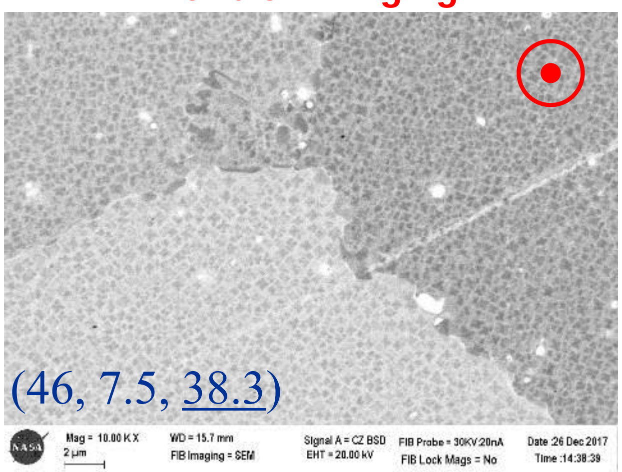

Supersolvus HT (+18ºC) for 2 h + Aging

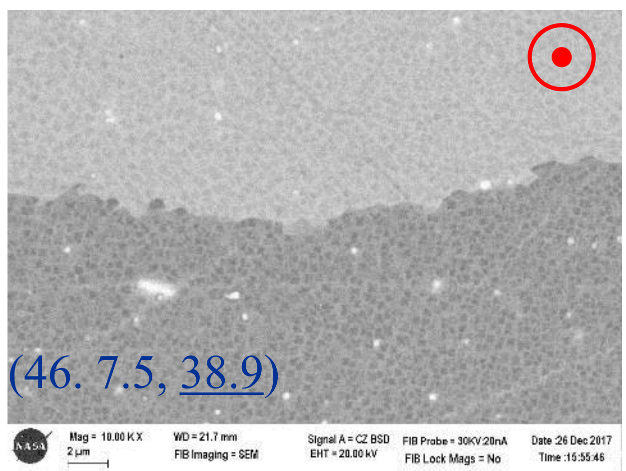

Supersolvus HT (+18ºC) for 4 h + Aging

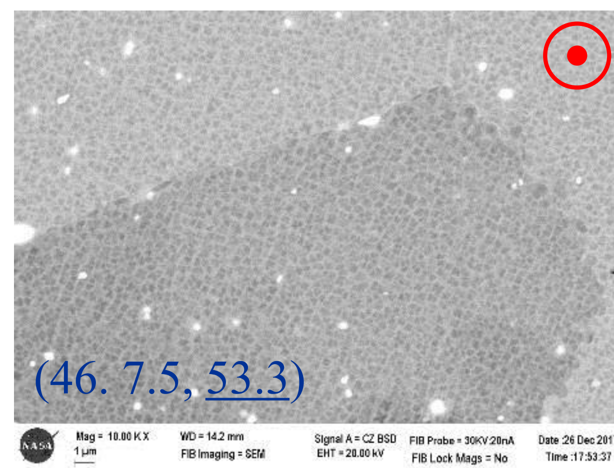

Center of Slab –Transverse Cross-Section

Concluding remarks

- EBM is promising for γ/γ' LSHR, which suggests good potential for EBM of other high γ'-volume fraction Ni-based superalloys
  - Excellent compositional consistency from build-to-build & throughout sample volume
  - Low porosity as-fabricated that is manageable with heat treatment and crack-free material is allowed by optimized processing even for large build elements (slabs)
- Coarser grain structure may necessitate to pivot application use
- EBM LSHR showed similarities to conventional PM LSHR:
  - Extraordinary fast cooling rates that led to fine dendritic structure with no secondary arm growth yet microsegregation
  - Similar microstructural response with carbides, borides and γ'-precipitates
- Subsolvus heat treatment led to undesirable features: bimodal precipitate size distribution and high density of fine grain colonies
- Supersolvus heat treat produced near equiaxed grains with reasonable heat treatment control despite larges grain sizes

Future Work

- Test mechanical behavior for comparisons to conventionally processed LSHR
  - In-plane vs. Z-direction
  - Tensile, creep, and fatigue at elevated temperatures

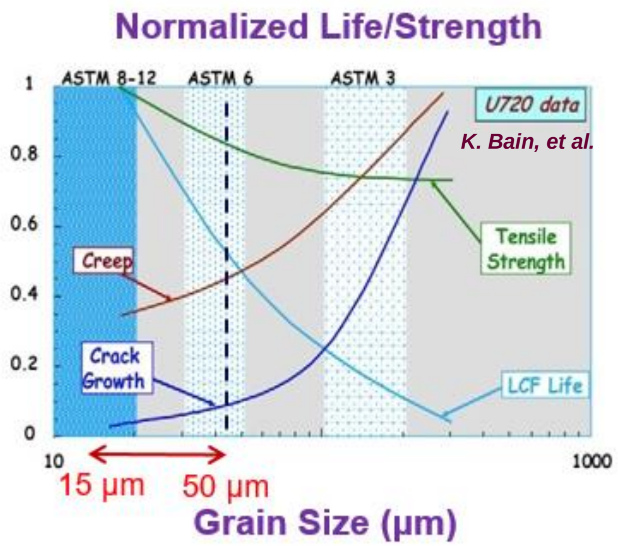

Thank you for your attention! Questions?